

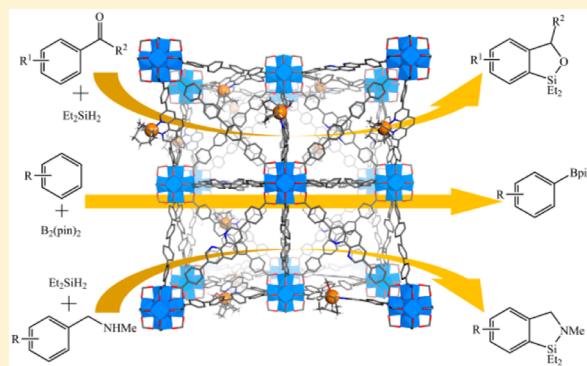
Bipyridine- and Phenanthroline-Based Metal–Organic Frameworks for Highly Efficient and Tandem Catalytic Organic Transformations via Directed C–H Activation

Kuntal Manna,[†] Teng Zhang,[†] Francis X. Greene, and Wenbin Lin*[‡]

Department of Chemistry, University of Chicago, 929 E 57th St., Chicago, Illinois 60637, United States

S Supporting Information

ABSTRACT: We report here the synthesis of a series of robust and porous bipyridyl- and phenanthryl-based metal–organic frameworks (MOFs) of UiO topology (BPV-MOF, mBPV-MOF, and mPT-MOF) and their postsynthetic metalation to afford highly active single-site solid catalysts. While BPV-MOF was constructed from only bipyridyl-functionalized dicarboxylate linker, both mBPV- and mPT-MOF were built with a mixture of bipyridyl- or phenanthryl-functionalized and unfunctionalized dicarboxylate linkers. The postsynthetic metalation of these MOFs with $[\text{Ir}(\text{COD})(\text{OMe})_2]$ provided Ir-functionalized MOFs (BPV-MOF-Ir, mBPV-MOF-Ir, and mPT-MOF-Ir), which are highly active catalysts for tandem dehydrosilylation of aryl ketones and aldehydes followed by dehydrogenative *ortho*-silylation of benzylicsilyl ethers as well as C–H borylation of arenes using B_2pin_2 . Both mBPV-MOF-Ir and mPT-MOF-Ir catalysts displayed superior activities compared to BPV-MOF-Ir due to the presence of larger open channels in the mixed-linker MOFs. Impressively, mBPV-MOF-Ir exhibited high TONs of up to 17000 for C–H borylation reactions and was recycled more than 15 times. The mPT-MOF-Ir system is also active in catalyzing tandem dehydrosilylation/dehydrogenative cyclization of *N*-methylbenzyl amines to azasilolanes in the absence of a hydrogen acceptor. Importantly, MOF-Ir catalysts are significantly more active (up to 95 times) and stable than their homogeneous counterparts for all three reactions, strongly supporting the beneficial effects of active site isolation within MOFs. This work illustrates the ability to increase MOF open channel sizes by using the mixed linker approach and shows the enormous potential of developing highly active and robust single-site solid catalysts based on MOFs containing nitrogen-donor ligands for important organic transformations.



INTRODUCTION

Bipyridines and phenanthrolines have been extensively employed in the construction of a wide variety of metal complexes with great potential in many applications ranging from catalysis to therapeutics.¹ In particular, owing to their robust redox stability, ease of functionalization, and entropically favored metal binding, these nitrogen donor-based chelating ligands have been routinely used in developing catalytic systems for solar energy conversion and fine chemical synthesis. However, homogeneous catalysts based on bipyridyl- and phenanthryl-derived ligands tend to have more open coordination environments than their phosphine counterparts, and as a result, they are more prone to deactivation via intermolecular pathways than metal-phosphine catalysts. To alleviate this drawback, steric protection around the metal centers using modified bulky bipyridyl- and phenanthryl-derived ligands is commonly employed to stabilize homogeneous single-site catalysts.² Installation of bulky substituents at the positions adjacent to the N-donors can significantly affect the ligand-binding properties as well as the electronic properties of metal–ligand complexes, which often attenuates the catalytic activities of the resulting metal complexes.³ Alternative

strategies are thus needed to engender enhanced stability and catalytic activity to homogeneous metal complex catalysts based on bipyridyl- and phenanthryl-derived ligands.

Over the past 15 years, metal–organic frameworks (MOFs) have emerged as an interesting class of porous molecular materials with great potential in many applications such as gas storage,⁴ separation,⁵ catalysis,⁶ nonlinear optics,⁷ chemical sensing,⁸ biomedical imaging,⁹ drug delivery,¹⁰ conductivity/semiconductivity,¹¹ and solar energy harvesting.¹² In particular, MOFs have been established as a highly tunable platform for developing single-site solid catalysts for various organic transformations.¹³ More recently, we showed that UiO-type MOFs provide an efficient means for stabilizing homogeneous catalysts based on simple bipyridyl and salicylaldimine ligands to afford much enhanced catalytic activity and even lead to catalytic activities that cannot be achieved with the homogeneous counterparts.¹⁴ As MOFs can be synthesized from well-defined molecular building blocks to tune their pore and channel sizes without change of MOF structures, further

Received: December 8, 2014

Published: February 2, 2015

synthetic elaborations of the bipyridyl- and phenanthryl-derived ligands can afford new MOF catalysts with much improved activities and efficiencies over the previously reported simple bipy-MOF.^{14a}

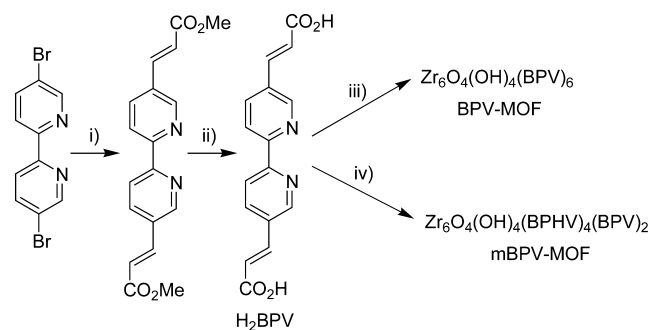
In this article, we report the design and synthesis of elongated bipyridyl- and phenanthryl-containing UiO MOFs with larger channels and their postsynthetic metalation with an iridium complex to afford highly active and efficient single-site solid catalysts for several important organic reactions via directed C–H activation. UiO-type MOFs built from $Zr_6(\mu_3-O)_4(\mu_3-OH)_4$ secondary building units (SBUs) and linear dicarboxylate linkers are highly stable under various reaction conditions and thus provide an ideal system for exploring catalytic applications.¹⁵ Furthermore, the UiO MOF topology is amenable to the incorporation of a wide variety of functionalities into the dicarboxylate linkers to lead to numerous novel functional materials for many important applications.¹⁶ A mixed linker strategy of using both the functionalized and unfunctionalized linkers was also developed in this work to afford mixed-linker MOFs with much larger open channels and pores to allow for facile diffusion of the substrates and products through the MOF channels. These Ir-functionalized MOFs have been employed as active, robust, and reusable solid catalysts in three important organic transformations: C–H borylation of arenes, tandem hydrosilylation of aryl ketones and aldehydes followed by hydroxyl-directed *ortho*-silylation, and tandem dehydrocoupling of *N*-methylbenzyl amines with Et_2SiH_2 to (hydrido)silyl amines and subsequent intramolecular dehydrogenative cyclization. Analogous homogeneous bipyridyl- and phenanthryl-iridium complexes were also prepared in order to compare their catalytic activities with those of the MOF-based catalysts. We demonstrate that the MOF-Ir catalysts are significantly more active than their homogeneous controls in both borylation and silylation reactions,¹⁷ revealing the crucial role of active site isolation within MOFs. Additionally, these solid MOF catalysts can overcome many fundamental difficulties associated with homogeneous catalysts such as capital- and labor-intensive ligand design in order to avoid multimolecular catalyst decomposition, leaching of toxic metal ions and complexes into the organic products, and the limitation of solvent choices due to poor solubility of some homogeneous catalysts in nonpolar solvents.

RESULTS AND DISCUSSION

BPV-MOF, mBPV-MOF, and mPT-MOF were constructed from both bipyridyl- or phenanthryl-functionalized dicarboxylate linker and the Zr-based SBU to afford UiO frameworks as shown in Schemes 1 and 2. The bipyridyl-containing dicarboxylate linker, H_2BPV , was synthesized from 5,5'-dibromo-2,2'-bipyridine in two steps (Scheme 1). The Heck coupling between 5,5'-dibromo-2,2'-bipyridine and methyl acrylate followed by saponification provided H_2BPV in 60% overall yield. The phenanthroline-containing dicarboxylate linker, H_2PT , was prepared from phenanthroline in three steps in a 22% overall yield (Scheme 2).

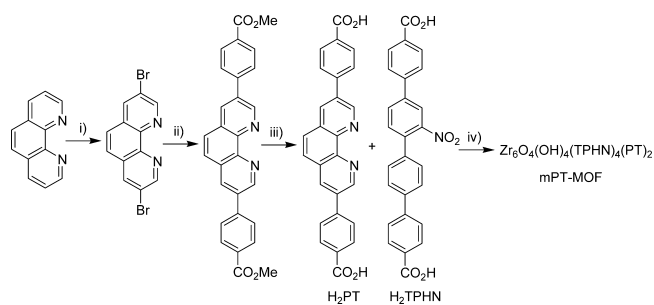
The solvothermal reaction between $ZrCl_4$ and H_2BPV in the presence of dimethylformamide (DMF) and trifluoroacetic acid (TFA) at 100 °C afforded BPV-MOF with a UiO framework of $Zr_6O_4(OH)_4(BPV)_6$ in 40% yield. In contrast, mBPV-MOF was synthesized in 40% yield by heating $ZrCl_4$ with H_2BPV and 4,4'-bis(carboxyethenyl)-1,1'-biphenyl (H_2BPHV) (in a 1:2 molar ratio) in the presence of DMF and TFA at 100 °C.

Scheme 1. Synthesis of BPV-MOF and mBPV-MOF^a



^aReagents: (i) methyl acrylate, $Pd(OAc)_2$, $P(o-tol)_3$, NEt_3 , DMF, 120 °C, 2 d; (ii) NaOH, EtOH, H_2O , reflux; (iii) $ZrCl_4$, DMF, TFA, 100 °C, 5 d; (iv) H_2BPHV , $ZrCl_4$, DMF, TFA, 100 °C, 5 d.

Scheme 2. Synthesis of mPT-MOF^a



^aReagents: (i) Br_2 , S_2Cl_2 , pyridine, *n*-BuCl, reflux, 12 h; (ii) 4-acetylphenylboronic acid, $Pd(PPh_3)_4$, CsF, DME, 100 °C, 3 d; (iii) aq NaOH, EtOH; (iv) $ZrCl_4$, DMF, TFA, 100 °C, 5 d.

Similarly, mPT-MOF was synthesized in 45% yield by heating $ZrCl_4$ and a mixture of H_2PT and 4,4'-bis(carboxyphenyl)-2-nitro-1,1'-biphenyl (H_2TPHN) in 1:2 molar ratio in a DMF solution in the presence of TFA at 100 °C. The presence of bipyridyl- and phenanthryl-containing dicarboxylate linkers in mBPV-MOF and mPT-MOF, respectively, was established and quantified by taking 1H NMR spectra of the digested MOFs. NMR studies consistently revealed that the ratio of biphenyl and bipyridine in the mBPV-MOF or the ratio of tetraphenyl and phenanthroline in mPT-MOF is approximately 2:1, corresponding to the molar ratio in the feed (Figures S6 and S10, Supporting Information [SI]). Nitrogen sorption measurements indicate that both mBPV-MOF and mPT-MOF are highly porous with a BET surface area of 1207 and 3834 m^2/g respectively (Figures S8 and S12, SI), and pore sizes of 7 and 7.7 Å, respectively (Figures S18 and S21, SI).

The structures of BPV-MOF and mBPV-MOF were established by comparing the powder X-ray diffraction (PXRD) patterns of the MOFs with the predicted pattern from a single-crystal structure of BPHV-MOF which was synthesized from $ZrCl_4$ and 4,4'-bis(carboxyethenyl)-1,1'-biphenyl (H_2BPHV) linker in the presence of DMF and TFA at 80 °C (Figure 1). A single-crystal X-ray diffraction study revealed that BPHV-MOF adopts the UiO structure (Figure 1a), with the $Zr_6(\mu_3-O)_4(\mu_3-OH)_4$ SBUs connected by the BPHV bridging linkers to afford the 12-connected *fcu* topology. However, BPHV-MOF crystallizes in a lower symmetry space group of $\bar{1}4$ due to the bending nature of the BPHV linker. The broadening of (101) peak and appearance of several other peaks suggest structural distortion in the powder samples,

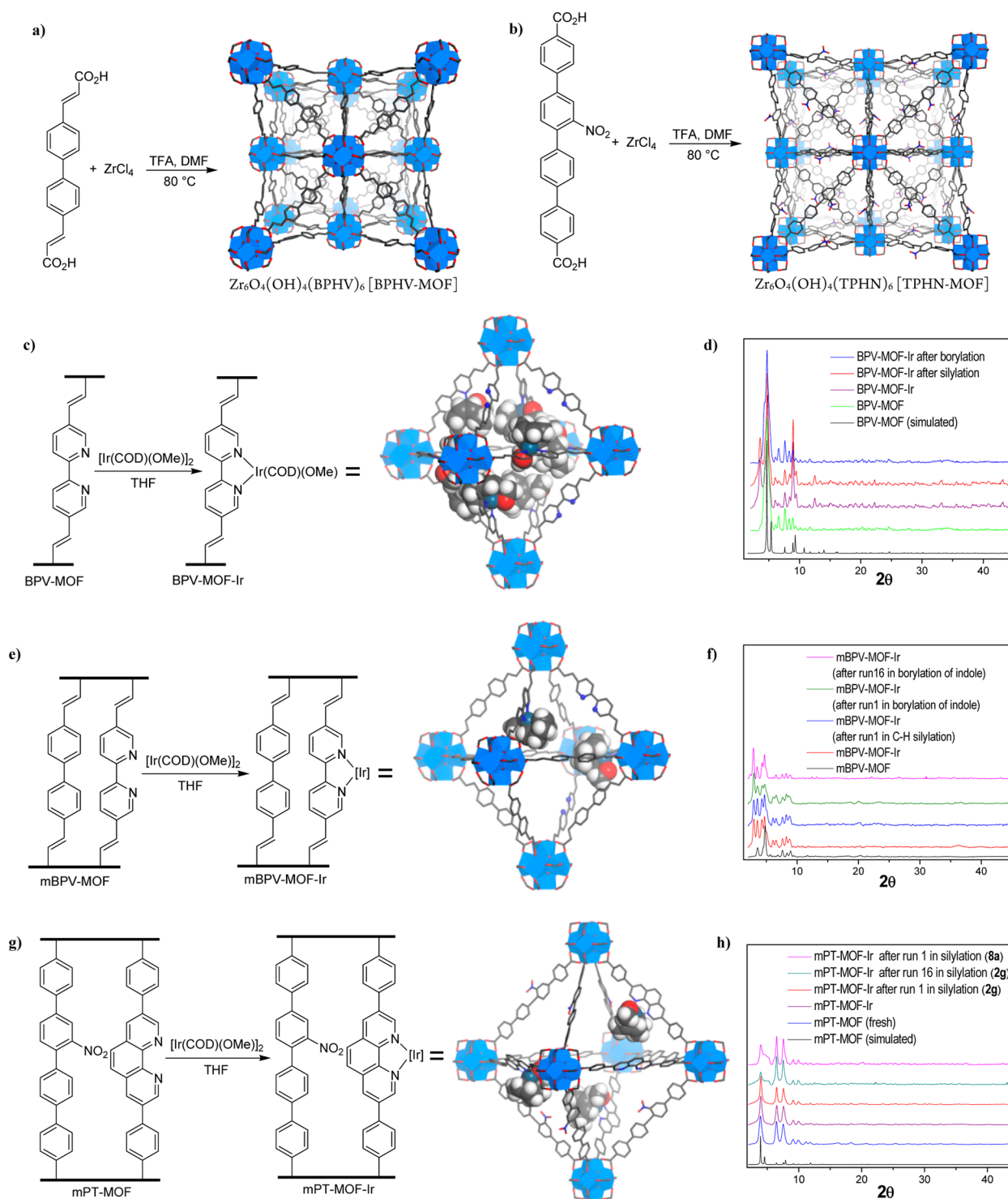


Figure 1. (a) Synthesis and single-crystal X-ray structure of BPHV-MOF. (b) Synthesis and single-crystal X-ray structure of TPHN-MOF. (c) Postsynthetic metalation of BPV-MOF. (d) PXRD patterns simulated from the cif file of BPHV-MOF (black) and of BPV-MOF (green), BPV-MOF-Ir (purple), BPV-MOF-Ir recovered from C–H silylation of **2a** (red), and BPV-MOF-Ir recovered from C–H borylation of *m*-xylene (blue). (e) Postsynthetic metalation of mBPV-MOF. (f) PXRD patterns of mBPV-MOF (black), mBPV-MOF-Ir (red), mBPV-MOF-Ir recovered from C–H silylation (blue), and mBPV-MOF-Ir recovered from C–H borylation of indole after run 1 (green) and after run 16 (pink). (g) Postsynthetic metalation of mPT-MOF. (h) PXRD patterns simulated from CIF file of TPHN-MOF (black) and of mPT-MOF (blue), mPT-MOF-Ir (purple), mPT-MOF-Ir recovered from C–H silylation of **2g** after run 1 (red) and after run 16 (green), and mPT-MOF-Ir recovered from amine-directed C–H silylation of **8a** after run 1 (pink).

which has been observed in other nanoscale MOFs.¹⁰ⁱ In the present case, the bent nature of the BPHV and BPV linkers provides additional mechanisms for structural distortions from the single-crystal structure. Similarly, the structure of mPT-

MOF was established by comparing the PXRD patterns with the simulated pattern from a single-crystal structure of TPHN-MOF which was synthesized from $ZrCl_4$ and 4,4'-bis(carboxyphenyl)-2-nitro-1,1'-biphenyl (H_2 TPHN) under sim-

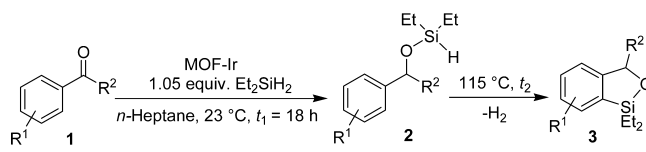
ilar conditions. TPHN-MOF adopts a typical UiO structure and crystallizes in the cubic $Fm\bar{3}m$ space group (Figure 1).

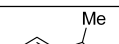
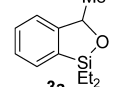
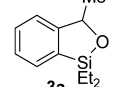
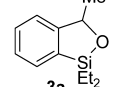
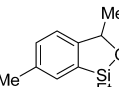
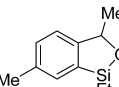
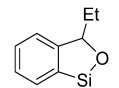
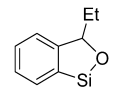
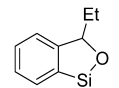
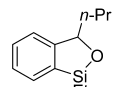
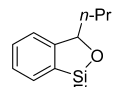
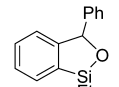
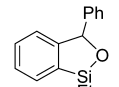
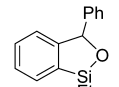
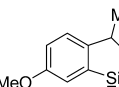
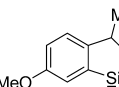
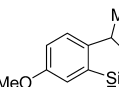
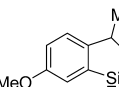
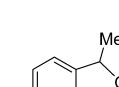
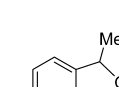
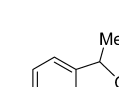
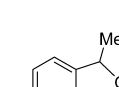
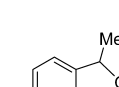
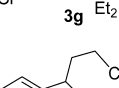
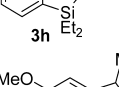
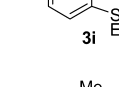
The postsynthetic metalation of BPV-MOF was performed by treating BPV-MOF with 2.0 equiv of $[\text{Ir}(\text{COD})(\text{OMe})_2]$ in THF to afford BPV-MOF-Ir as a deep purple solid (Figure 1c). Similarly, mBPV-MOF-Ir and mPT-MOF-Ir were prepared as a deep purple and deep green solid, respectively, by the treatment of mBPV-MOF and mPT-MOF with 1.0 equiv of $[\text{Ir}(\text{COD})(\text{OMe})_2]$ in THF (Figure 1e,g), respectively. Inductively coupled plasma-mass spectroscopy (ICP-MS) analyses of Ir/Zr ratio of the digested metalated MOFs revealed the Ir loadings of 65%, 16%, and 20% with respect to the Zr centers for BPV-MOF-Ir, mBPV-MOF-Ir, and mPT-MOF-Ir, respectively. mPT-MOF was also metalated with $[\text{IrCl}(\text{COD})_2]$ in THF to obtain mPT-MOF-Ir(COD)-Cl as a green solid at a 12% Ir loading. Because mBPV-MOF-Ir and mPT-MOF-Ir only contain one-third functionalized linkers, these Ir loadings correspond to the metalation of 48% and 61% of the BPV and PT linkers in these mMOFs. The crystallinity of all the MOFs was maintained upon metalation as shown by similar PXRD patterns of MOFs and MOF-Ir materials (Figure 1d,f,h). BPV-MOF-Ir, mBPV-MOF-Ir, and mPT-MOF-Ir have BET surface area of 106, 563, and 1828 m^2/g , respectively, and pore sizes of 5.8, 5.9, and 6.7 Å, respectively. The smaller surface areas and pore sizes of metalated MOFs compared to their pristine analogs are due to the presence of Ir and associated ligands in the MOF cavities.

We performed homogeneous control experiments in order to identify the Ir species formed from postsynthetic metalation of the MOFs. Treatment of $[\text{Ir}(\text{COD})(\text{OMe})_2]$ with H_2BPV or Me_2BPV at room temperature afforded $(\text{H}_2\text{BPV})\text{Ir}(\text{COD})(\text{OMe})$ and $(\text{Me}_2\text{BPV})\text{Ir}(\text{COD})(\text{OMe})$, respectively. The identities of both Ir complexes were established by NMR spectroscopy and mass spectrometry. These Ir complexes are air- and water-sensitive and rapidly decomposed under MOF digestion conditions. However, because H_2BPV or Me_2BPV ligands were completely metalated to form $(\text{H}_2\text{BPV})\text{Ir}(\text{COD})(\text{OMe})$ or $(\text{Me}_2\text{BPV})\text{Ir}(\text{COD})(\text{OMe})$ at room temperature, we can infer that the identities of the Ir species in the metalated MOFs as $\text{Ir}(\text{L})(\text{COD})(\text{OMe})$ (L= BPV or PT) complexes.

BPV-MOF-Ir, mBPV-MOF-Ir, and mPT-MOF-Ir are all active in catalyzing the hydrosilylation of aryl ketones to benzylicsilyl ethers and subsequent intramolecular *ortho*-silylation of benzylicsilyl ethers to give benzoxasiloles (Table 1).¹⁸ Benzoxasiloles are important in organic synthesis and can be converted to phenols by Tamao–Fleming oxidation^{18,19} or to biaryl derivatives by Hiyama cross-coupling reactions.²⁰ In homogeneous catalysis pioneered by Hartwig and co-workers, the hydrosilylation of ketones was catalyzed by $[\text{Ir}(\text{COD})(\text{OMe})_2]$, and the subsequent intramolecular *ortho*-silylation of benzylicsilyl ethers was catalyzed by phenanthroline-derived Ir(I) complex in the presence of norbornene as the hydrogen acceptor.^{18,21} This homogeneous reaction requires relatively high catalyst loadings and the use of a hydrogen acceptor. In MOF-Ir-catalyzed silylation reactions, the hydrosilylation of ketones proceeded at room temperature, but the dehydrogenative *ortho*-silylation of benzylicsilyl ethers required elevated temperatures. Screening experiments revealed that the intramolecular *ortho*-silylation gave the highest turnover frequency when the reaction mixture was refluxed in *n*-heptane under nitrogen atmosphere at 115 °C (Table S2 and Figure S25, SI). At 0.1 mol % Ir loading, BPV-MOF-Ir provided benzylicsilyl ether **2a** in complete conversion upon treatment of

Table 1. MOF-Ir-Catalyzed Tandem Hydrosilylation of Ketones and Intramolecular *ortho*-Silylation of Benzylicsilyl Ethers to Afford Benzoxasiloles^a



Entry	Product	MOF-Ir catalyst (mol% loading)	Time (t_2)	Yield (%) ^b
1		BPV-MOF (0.1)	8 d	72
2		mBPV-MOF (0.1)	8 d	100 (93)
3		mPT-MOF (1.0)	24 h	100
4		mPT-MOF (0.1)	7 d	100 (86)
5		mBPV-MOF (0.1)	5 d	100 (95)
6		mPT-MOF (0.1)	4 d	100 (94)
7		BPV-MOF (0.1)	7 d	100
8		mBPV-MOF (0.1)	2.5 d	100 (94)
9		mPT-MOF (0.1)	2.5 d	100 (95)
10		mBPV-MOF (0.1)	5 d	100 (96)
11		mPT-MOF (0.1)	4.5 d	100 (94)
12		mBPV-MOF (0.1)	3 d	100
13		mPT-MOF (1.0)	15 h	100 (97)
14		mPT-MOF (0.1)	7 d	100
15		BPV-MOF (0.1)	5 d	26
16		mBPV-MOF (0.1)	3.5 d	100
17		mPT-MOF-Ir (1.0)	15 h	100
18		mPT-MOF (0.1)	4.5 d	100 (89)
19		BPV-MOF (0.1)	6 d	100 (96)
20		mBPV-MOF (0.1)	40 h	100 (96)
21		mPT-MOF (0.1)	35 h	100 (94)
22		mPT-MOF (0.05)	4 d	100 (91)
23		mPT-MOF (0.025)	8 d	76
24		mPT-MOF (0.1)	3 d	100
25		mPT-MOF (0.1)	2 d ^c	100
26		mPT-MOF (0.1)	17 d ^d	100 (93)

^aReaction conditions: 5.0 mg of MOF-Ir (0.1 mol % Ir) or other loadings as specified, 4.0 mL of *n*-heptane, 115 °C, reflux under N_2 .

^bIsolated yield in the parentheses. ^c $t_1 = 42$ h. ^d $t_1 = 4$ d.

acetophenone with 1.05 equiv Et_2SiH_2 in *n*-heptane for 18 h at room temperature. Refluxing the resultant mixture at 115 °C for 8 d afforded corresponding benzoxasilole **3a** with 72% conversion. Under identical reaction conditions, 0.1 mol % mBPV-MOF-Ir and mPT-MOF-Ir gave complete conversions of **2a** and afforded **3a** in good isolated yields (Table 1, entries 2 and 4). The dehydrogenative *ortho*-silylation of benzylicsilyl ethers was accompanied by the generation of a stoichiometric

amount of H₂, which was identified and quantified by GC analysis (Figure S27, SI). Importantly, no H₂ acceptor was needed, which represents an improvement over the reported homogeneous C–H silylation reactions in terms of atom economy. The PXRD patterns of MOFs recovered from the silylation reactions remained the same as those of freshly prepared MOF-Ir precatalysts, indicating that the MOF frameworks are stable under the catalytic conditions (Figure 1d,f,h). The higher catalytic activities of both mBPV-MOF-Ir and mPT-MOF-Ir compared to BPV-MOF-Ir were also observed for other substrates (Table 1; entries 7–9, 15–18, 19–21). The enhanced activity of mMOF catalysts compared to BPV-MOF-Ir is likely due to the presence of more open channels, which facilitates diffusion of substrates and products through the channels of mMOFs. Directly refluxing a mixture of acetophenone and Et₂SiH₂ in *n*-heptane at 115 °C using 0.1 mol % of mPT-MOF-Ir resulted in the complete conversion of **1a**, however, afforded benzoxasilole **3a** in a lower yield (82%), presumably due to the decomposition of the Ir-hydride intermediate generated during the hydrosilylation step at higher temperatures.

Tandem hydrosilylation of aryl ketones and intramolecular *ortho*-silylation reactions catalyzed by mBPV-MOF-Ir and mPT-MOF-Ir have a broad substrate scope as shown in Table 1. At 0.1 mol % Ir loading, mixed-linker MOFs gave complete conversions of both the aryl ketones (**1a–j**) and the *in situ* generated benzylicsilyl ethers (**2a–j**) in absence of hydrogen acceptor to afford benzoxasiloles (**3a–j**) in excellent yields (86–100%). Monoalkyl (**3a–d**), aryl (**3e**), alkoxy (**3f** and **3i**), and halogen (**3g–h**) substituents were all tolerated under the reaction conditions. Benzoxasiloles could also be prepared from *sec*-benzyl alcohols by dehydrocoupling of alcohols to benzylicsilyl ethers at room temperature, followed by intramolecular cyclization at 115 °C. For example, **3c** was afforded from 1-phenyl-1-propanol (**1c**) in 94% and 95% yields for mBPV-MOF-Ir and mPT-MOF-Ir, respectively (Table 1, entries 8 and 9). Additionally, heteroaromatic benzoxasilole (**3j**) was also obtained in 93% yield with 0.1 mol % of mPT-MOF-Ir (Table 1, entry 26). Notably, a turnover number (TON) of 3200 was observed for mPT-MOF-Ir with **1g** as the substrate (Table 1, entry 23).

Ir-functionalized mixed-linker MOFs are also active in catalyzing hydrosilylation of benzaldehydes (**4**) and *in situ* cyclization of the primary (hydrido)silyl ethers (**5**) under identical reaction conditions to those for aryl ketones (Table 2). Although longer reaction times were required in both steps, full conversions were observed, and excellent yields of benzoxasiloles (**6**) were obtained with 0.5 mol % mBPV-MOF-Ir and mPT-MOF-Ir catalysts. Notably, both mBPV-MOF-Ir and mPT-MOF-Ir catalysts are significantly more active in intramolecular *ortho*-silylation of benzylicsilyl ethers than their homogeneous control analogs. Under identical conditions, 0.5 mol % of {pth}Ir(COD)(OMe) {pth = 3,8-bis(4-methoxycarbonylphenyl)phenanthroline} afforded **6b** in only 37% conversion in 3 d, after which no further conversion was observed with further heating. In contrast, the conversion of **5b** proceeded linearly with time until completion in the presence of 0.2 mol % of the mPT-MOF-Ir catalyst (Figure 2a). This result indicates that mPT-MOF-Ir is at least 7 times more active than the homogeneous control for the intramolecular silylation reaction. Time-dependent GC conversion curves indicated that mBPV-MOF-Ir was also at least 3 times more active than its homogeneous control [bpy(CH=

Table 2. mBPV-MOF-Ir- and mPT-MOF-Ir-Catalyzed Tandem Hydrosilylation of Aldehyde and Intramolecular *ortho*-Silylation of Benzylicsilyl Ethers to Prepare Benzoxasiloles^a

entry	R	MOF-Ir	time, t ₂ (d)	yield (%) ^b
1	H	mBPV-MOF-Ir	4.5	100
2		mPT-MOF-Ir	3	100 (95)
3	Cl	mBPV-MOF-Ir	4	100 (96)
4		mPT-MOF-Ir	3.5	100 (86)
5	Br	mPT-MOF-Ir	4.5	100

^aReaction conditions: MOF-Ir (0.5 mol % Ir), 4.0 mL *n*-heptane, 115 °C, reflux under N₂. ^bIsolated yield in the parentheses.

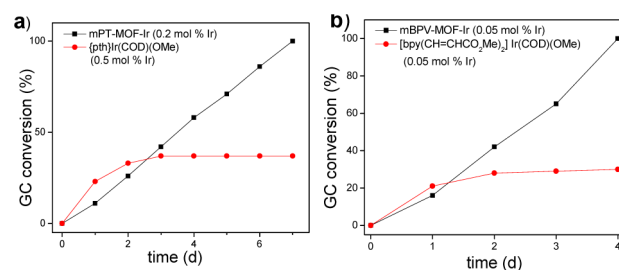


Figure 2. (a) Plots of GC conversion (%) vs time for *ortho*-silylation of **5b** using mPT-MOF-Ir (0.2 mol %) and {pth}Ir(COD)(OMe) (0.5 mol %) as catalysts in *n*-heptane at 115 °C. (b) Plots of GC conversion (%) vs time for *ortho*-silylation of **2g** using mBPV-MOF-Ir (0.05 mol %) and [bpy(CH=CHCO₂Me)₂]Ir(COD)(OMe) (0.05 mol %) as catalysts in *n*-heptane at 115 °C.

CHCO₂Me)₂]Ir(COD)(OMe) (Figure 2b). The higher activities of MOF catalysts strongly support the beneficial effect of active site isolation in the MOF framework, which prevents any intermolecular deactivation pathways.

Remarkably, at a 0.5 mol % Ir loading, mPT-MOF-Ir could be recovered and reused for the intramolecular *ortho*-silylation of **2g** at least 15 times without loss of MOF crystallinity (Figures 3 and 1f). Excellent yields (86–99%) of the benzoxasilole, **3g**, were obtained consistently in the reuse experiments. Importantly, **3g** was obtained in high purity

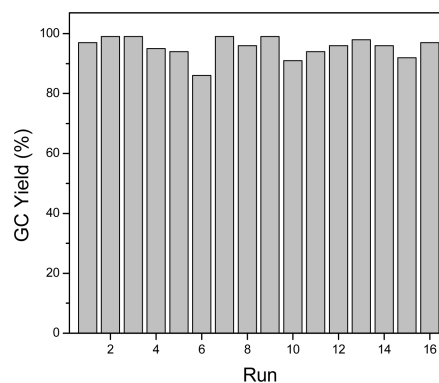
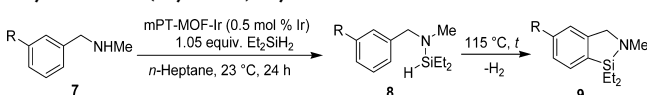


Figure 3. Plot of yield (%) of benzoxasilole at various runs in the recycle and reuse of mPT-MOF-Ir (0.5 mol % Ir) for *ortho*-silylation of **2g**.

simply by removing the solid catalyst and the organic volatiles (without any other workup). The heterogeneous nature of mPT-MOF-Ir was further confirmed by several experiments. The PXRD patterns of mPT-MOF-Ir recovered from the first and 16th run remained essentially unchanged from that of freshly prepared mPT-MOF-Ir (Figure 1h). Additionally, ICP-MS analyses showed that the amounts of Ir and Zr leaching into the supernatant after the first run were 2.1% and 0.008%, respectively, and the amounts of leached Ir and Zr after the fifth run were 0.08% and 0.009%, respectively. Moreover, no further conversion was detected after removal of mPT-MOF-Ir during the course of the silylation reaction (Scheme S1, SI). These results collectively indicate that the mPT-MOF-Ir catalyst is very stable under the catalytic conditions.

The high activity of mPT-MOF-Ir in hydroxyl-directed intramolecular silylation of arene C–H bonds inspired us to investigate the analogous silylation reactions directed by an amine group. The dehydrogenative intramolecular silylation of aromatic C–H bonds of (hydrido)silyl amines would generate azasilolanes. The silicon-heteroatom bonds in azasilolanes could be further functionalized via oxidation or halogenations. Recently, Hartwig and co-workers reported Ir-catalyzed secondary amine-directed silylation of aromatic C–H bonds, in which (hydrido)silyl amines, generated *in situ* by [Ir(COD)(OMe)₂]-catalyzed dehydrocoupling of benzylamine with Et₂SiH₂, undergo dehydrogenative silylation in the presence of norbornene as the hydrogen acceptor by 3,4,7,8-tetramethyl-1,10-phenanthroline-derived iridium catalyst.²² Interestingly, mPT-MOF-Ir afforded azasilolanes directly from *N*-methylbenzyl amines and Et₂SiH₂ without employing any hydrogen acceptor. Analogous to hydroxyl-directed silylation reactions, 0.5 mol % mPT-MOF-Ir provided (hydrido)silyl amines in *n*-heptane at room temperature in 24 h. Refluxing the resultant mixture at 115 °C afforded azasilolanes in complete conversions (Table 3). Azasilolanes **9a** and **9b** were obtained in

Table 3. mPT-MOF-Ir-Catalyzed Tandem Dehydrocoupling of *N*-Methylbenzyl Amines and Intramolecular *ortho*-Silylation of (Hydrido)silyl Amines to Azasilolanes^a



entry	R	time, <i>t</i>	conversion (%) ^b
1	H (9a)	6 d	100 (92)
2	Cl (9b)	10 d	100 (82)

^aReaction conditions: mPT-MOF-Ir (0.5 mol % Ir), 4.0 mL *n*-heptane, 115 °C, reflux under N₂. ^bNMR yield in the parentheses.

92% and 82% yields respectively (Table 3, entries 1 and 2). In contrast, 0.5 mol % of {pth}Ir(COD)(OMe) afforded **9a** from **8a** in only 20% conversion at 115 °C in *n*-heptane, and no further conversion was observed upon refluxing for longer times. The similar PXRD pattern of recovered mPT-MOF-Ir to that of freshly prepared catalyst indicates that the MOF remained crystalline and stable under the reaction conditions (Figure 1h).

MOF-Ir catalysts are also active in dehydrogenative borylation of aromatic C–H bonds using B₂(pin)₂ (pin = pinacolate) as the borylating agent.²³ Borylation of aryl C–H bonds provides aryl boronates, which are versatile reagents in organic synthesis.²⁴ In homogeneous catalysis, a number of nitrogen and phosphine-based iridium(I) catalysts have been

reported, and generally bipyridyl-derived catalysts are more active compared to those containing phosphine ligands. Recently, efforts to develop heterogeneous borylation catalysts have been made based on iridium(0) nanoparticles,²⁵ insoluble iridium complex,²⁶ or silica-supported catalyst.²⁷ The MOF-Ir-catalyzed borylation reactions were first screened for optimized conditions such as temperature, solvents, and in neat arenes (without using a solvent) to obtain the best results. The screening experiments revealed that the highest turnover frequencies were observed when the borylation reactions were performed in neat arene at 115 °C or refluxed in *n*-heptane at 115 °C for solid substrates (Tables S3 and S4; SI). Longer reaction time was required when the reaction mixture was heated above 115 °C, which is likely due to the instability of active catalytic species at higher temperatures. Under the optimized conditions, 0.1 mol % BPV-MOF-Ir gave 72% of 5-(4,4,5,5-tetramethyl-1,3,2-dioxaborolan-2-yl)-*m*-xylene (**11a**) in 5 d from *m*-xylene and 100% of 2-(4,4,5,5-tetramethyl-1,3,2-dioxaborolan-2-yl)-1H-indole (**11h**) from indole in 16 h (Table 4, entries 1 and 15). In contrast, mBPV-MOF-Ir and mPT-MOF-Ir afforded **11a** and **11h** in quantitative yields at much shorter reaction times (Table 4; entries 2, 4, 16, and 18). mPT-MOF-Ir(COD)-Cl was about half as active in C–H borylation as mPT-MOF-Ir. The TPHN-MOF treated with [Ir(COD)(OMe)₂] did not give any activity for benzene borylation, ruling out the involvement of the Zr₆(μ₃-O)₄(μ₃-OH)₄ SBUs in arene borylation reactions. The faster reaction rates due to the presence of more open channels within the mMOF-Ir catalysts led us to investigate the borylation reactions with a broad range of substrates. Monoborylated arenes were obtained in excellent yields (94–100%) for a range of activated and unactivated arenes (Table 4). Halogen and alkoxy functional groups were well tolerated under the reaction conditions. The regioselectivities of borylated products are the same as those reported for homogeneous Ir catalysts.^{23b,d} The borylation occurred at the least sterically hindered C–H bonds of the unactivated arenes (Table 4, entries 1–14) and at the 2-position of heteroarenes such as indole and benzo[*b*]furan (Table 4, entries 15–19). Notably, pure products were obtained by simply removing the catalyst via centrifugation followed by removal of the volatiles. Although both mMOFs afforded borylated arenes in excellent yields, mBPV-MOF-Ir displayed superior activity over mPT-MOF-Ir. Importantly, TONs of 17000 and 9000 were obtained for borylation of *m*-xylene and indole, respectively, with mBPV-MOF-Ir (Table 1; entries 3 and 17). In these two cases, the leached iridium contents in 5-(4,4,5,5-tetramethyl-1,3,2-dioxaborolan-2-yl)-*m*-xylene (**11a**, 1.50 g, 6.46 mmol) and 2-(4,4,5,5-tetramethyl-1,3,2-dioxaborolan-2-yl)-1H-indole (**11h**, 0.765 g, 3.15 mmol) were 1.22 and 0.3 ppm, respectively. Therefore, pure borylated products containing very low residual iridium in 1 ppm or lower levels could be obtained without any chromatographic purification.

Interestingly, both mMOFs catalysts are significantly more active in C–H borylation of arenes than their homogeneous counterparts. Time-dependent GC conversion curves indicated that mBPV-MOF-Ir was also at least 95 times more active than its homogeneous control [bpy(CH=CHCO₂Me)₂]Ir(COD)(OMe) (Figure 4a). [bpy(CH=CHCO₂Me)₂]Ir(COD)(OMe) had a very low activity in borylation reaction. At 115 °C in neat *m*-xylene, 0.05 mol % [bpy(CH=CHCO₂Me)₂]Ir(COD)(OMe) afforded **8a** in only 9% conversion after 2 d, and then no further conversion was observed with prolonged

Table 4. MOF-Ir-Catalyzed C–H Borylation of Arenes^a

Entry	Substrate	Product	MOF-Ir catalyst	Ir loading (mol %)	Time	Yield (%) ^b
1 ^c			BPV-MOF-Ir	0.1	5 d	72
2 ^c			mBPV-MOF-Ir	0.1	16 h	100 (97)
3 ^c			mBPV-MOF-Ir	0.005	15 d	85
4 ^c			mPT-MOF-Ir	0.1	32 h	100 (96)
5 ^c			mBPV-MOF-Ir	0.1	16 h	100 (97)
6 ^c			mPT-MOF-Ir	0.1	35 h	100 (99)
7 ^c			mBPV-MOF-Ir	0.1	16 h	100
8 ^c			mPT-MOF-Ir	0.1	18 h	100
9 ^c			mPT-MOF-Ir	0.1	18 h	100 (<i>o:m:p</i> = 0.62:38)
10 ^c			mBPV-MOF-Ir	0.1	24 h	100 (94)
11 ^c			mPT-MOF-Ir	0.1	30 h	100 (95)
12			mPT-MOF-Ir	1.0	24 h	100
13			mBPV-MOF-Ir	0.1	36 h	100 (96)
14			mPT-MOF-Ir	0.1	2 d	100
15			BPV-MOF-Ir	0.1	18 h	100
16			mBPV-MOF-Ir	0.1	5 h	100 (98)
17			mBPV-MOF-Ir	0.01	9 d	90
18			mPT-MOF-Ir	0.1	11 h	100 (94)
19			mPT-MOF-Ir	0.5	18 h	100

^aReaction conditions: MOF-Ir, 0.508 mmol B₂pin₂, 1.02 mmol of arene, 3.0 mL of *n*-heptane, 115 °C, reflux under N₂. ^bIsolated yield in the parentheses. ^cNeat arene was used.

heating. However, under identical conditions, mBPV-MOF-Ir gave **11a** with a TON of 17000. mPT-MOF-Ir also compares favorably to its homogeneous counterpart, with at least twice as high activity as its homogeneous control (Figure S32, SI). Therefore, immobilization of molecular catalysts in the MOF framework dramatically enhances the overall activity and stability of the catalysts by preventing bimolecular deactivation pathways. Remarkably, at a 0.5 mol % Ir loading, the MOF-Ir catalyst was reused more than 15 times in the borylation of indole without loss of catalytic activity (Figure 4b) or MOF crystallinity (Figure 1f). Excellent yields (89–100%) of 2-(4,4,5,5-tetramethyl-1,3,2-dioxaborolan-2-yl)-1H-indole (**11h**) were obtained consistently in the reuse experiments. Notably, **11h** was obtained in high purity simply by removing the solid catalyst and the organic volatiles. The heterogeneity of mBPV-MOF-Ir was confirmed by several experiments. The PXRD patterns of mBPV-MOF-Ir recovered from the first and 16th run remained the same as that of freshly prepared mBPV-MOF-Ir (Figure 1f), indicating that the MOF catalyst is very stable under the catalytic conditions. The leaching of Ir and Zr into the supernatant was very low during the course of the

borylation reaction as shown by ICP-MS analysis. The amounts of Ir and Zr leaching into the supernatant after the first run were 0.132% and 0.029%, respectively, and after the fifth run were 0.016% and 0.012%, respectively. Moreover, no further conversion was detected after removal of mBPV-MOF-Ir from the reaction mixture (Scheme S5, SI). mPT-MOF-Ir could also be recycled 15 times for borylation of *m*-xylene (Figure 4c). The PXRD of recovered mPT-MOF-Ir after run 17 indicated that the MOF remained crystalline, which suggests that the deactivation of mPT-MOF-Ir at run 17 is due to the decomposition of the active Ir-catalyst but not the MOF framework. Additionally, ICP-MS analyses showed that the amounts of Ir and Zr leaching into the supernatant were 0.042% and 0.038%, respectively, after the first run, 0.08% and 0.009%, respectively, after the fifth run, and 0.018% and 0.014%, respectively, after the 10th run.

CONCLUSIONS

We have constructed three porous Zr-MOFs (BPV-MOF, mBPV-MOF, and mPT-MOF) of UiO topology with elongated bipyridyl- and phenanthryl-containing bicarboxylate linkers.

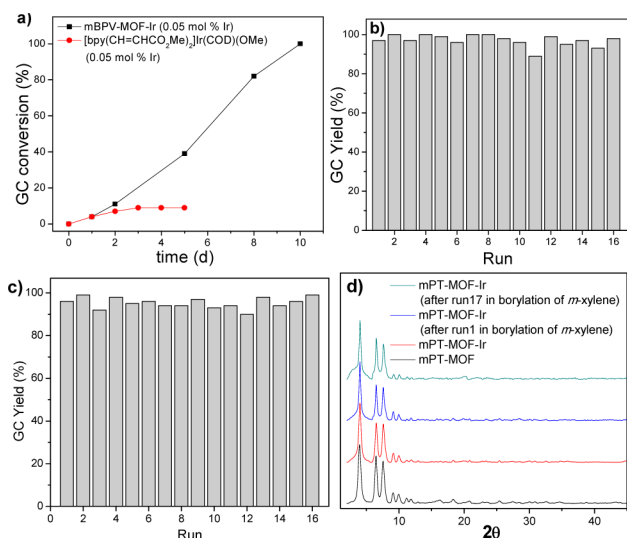


Figure 4. (a) Plots of GC conversion (%) vs time (h) for C–H borylation of *m*-xylene using mBPV-MOF-Ir (0.01 mol %) and [bpy(CH=CHCO₂Me)₂]Ir(COD)(OMe) (0.05 mol %) as catalysts under identical conditions. (b) Plots of GC conversion (%) vs time (h) for various runs in the recycle and reuse of mBPV-MOF-Ir for borylation of indole. (c) Plots of GC conversion (%) vs time (h) for various runs in the recycle and reuse of mPT-MOF-Ir for borylation of *m*-xylene. (d) PXRD patterns of freshly prepared mPT-MOF (black), mPT-MOF-Ir (red), and mPT-MOF-Ir recovered from C–H borylation of *m*-xylene after run 1 (blue) and after run 17 (green).

The straightforward postsynthetic metalation of these UiO-MOFs with [Ir(COD)(OMe)₂] afforded highly active and robust single-site solid catalysts for three important organic transformations via directed C–H activation: tandem hydrosilylation/*ortho*-silylation of aryl ketones and aldehydes, tandem dehydrocoupling/*ortho*-silylation reactions of *N*-methylbenzyl amines, and borylations of aromatic C–H bonds. In all three reactions, mixed-linker MOF catalysts (mMOF-Ir) are much more active than BPV-MOF containing only functionalized linkers. We believe that mMOF catalysts have much larger open channels due to the doping of bulky functionalized linkers and their resulting Ir complexes into less sterically demanding unfunctionalized linkers, which facilitates the transport of the substrates and products through the MOF channels. We have also observed that mMOF catalysts show much enhanced activities and stability when compared to their homogeneous analogues, likely due to active site isolation in MOF structures which prevents any intermolecular deactivation pathways. In addition, these solid catalysts can be readily recycled and reused for more than 15 times. Our work thus introduces a simple and efficient doping strategy to enlarge the open channels of catalytically active MOFs and highlights the enormous potential of developing MOF catalysts based on nitrogen-donor ligands for practical synthesis of fine chemicals.

■ ASSOCIATED CONTENT

Supporting Information

General experimental section; synthesis and characterization of BPV-MOF, mBPV-MOF, mPT-MOF, BPV-MOF-Ir, mBPV-MOF-Ir, and mPT-MOF-Ir; procedures for BPV-MOF-Ir, mBPV-MOF-Ir, and mPT-MOF-Ir-catalyzed C–H borylation of arenes, tandem hydrosilylation and intramolecular *ortho*-silylation of benzylsilyl ethers, and tandem dehydrocoupling and intramolecular *ortho*-silylation of (hydrido)silyl amines;

recycle procedure of mBPV-MOF-Ir and mPT-MOF-Ir in C–H borylation of arenes and intramolecular *ortho*-silylation of benzylsilyl ethers; GC analysis conditions for all products. This material is available free of charge via the Internet at <http://pubs.acs.org>.

■ AUTHOR INFORMATION

Corresponding Author

*wenbinlin@uchicago.edu

Author Contributions

†These authors contributed equally.

Notes

The authors declare no competing financial interest.

■ ACKNOWLEDGMENTS

This work was supported by NSF (CHE-1111490) and startup funds from the University of Chicago. We thank Dr. Michaël Carboni, Dr. Takahiro Sawano, and Dr. Nathan C. Thacker for experimental help, Christopher Poon, Zekai Lin, and Carter W. Abney for performing ICP-MS experiments, and Kuangda Lu for taking TEM images. Single-crystal diffraction studies were performed at ChemMatCARS (Sector 15), APS, Argonne National Laboratory. ChemMatCARS is principally supported by the NSF Divisions of Chemistry and Materials Research (CHE-1346572). Use of the Advanced Photon Source, an Office of Science User Facility operated for the U.S. DOE Office of Science by ANL, was supported by the U.S. DOE under contract no. DE-AC02-06CH11357.

■ REFERENCES

- (1) (a) Fussa-Rydel, O.; Zhang, H. T.; Hupp, J. T.; Leidner, C. R. *Inorg. Chem.* **1989**, *28*, 1533. (b) Chalk, S. J.; Tyson, J. F. *Anal. Chem.* **1994**, *66*, 660. (c) Balzani, V.; Juris, A.; Venturi, M.; Campagna, S.; Serroni, S. *Chem. Rev.* **1996**, *96*, 759. (d) Bachas, L. G.; Cullen, L.; Hutchins, R. S.; Scott, D. L. *J. Chem. Soc., Dalton Trans.* **1997**, 1571. (e) Chow, C. S.; Bogdan, F. M. *Chem. Rev.* **1997**, *97*, 1489. (f) Kaes, C.; Katz, A.; Hosseini, M. W. *Chem. Rev.* **2000**, *100*, 3553. (g) Chelucci, G.; Thummel, R. P. *Chem. Rev.* **2002**, *102*, 3129.
- (2) Sampson, M. D.; Nguyen, A. D.; Grice, K. A.; Moore, C. E.; Rheingold, A. L.; Kubiak, C. P. *J. Am. Chem. Soc.* **2014**, *136*, 5460.
- (3) Obligation, J. V.; Chirik, P. J. *Org. Lett.* **2013**, *15*, 2680.
- (4) (a) Eddaoudi, M.; Kim, J.; Rosi, N.; Vodak, D.; Wachter, J.; O’Keeffe, M.; Yaghi, O. M. *Science* **2002**, *295*, 469. (b) Rosi, N. L.; Eckert, J.; Eddaoudi, M.; Vodak, D. T.; Kim, J.; O’Keeffe, M.; Yaghi, O. M. *Science* **2003**, *300*, 1127. (c) Murray, L. J.; Dinca, M.; Long, J. R. *Chem. Soc. Rev.* **2009**, *38*, 1294. (d) Suh, M. P.; Park, H. J.; Prasad, T. K.; Lim, D.-W. *Chem. Rev.* **2012**, *112*, 782. (e) Gassensmith, J. J.; Furukawa, H.; Smaldone, R. A.; Forgan, R. S.; Botros, Y. Y.; Yaghi, O. M.; Stoddart, J. F. *J. Am. Chem. Soc.* **2011**, *133*, 15312.
- (5) (a) Chen, B.; Liang, C.; Yang, J.; Contreras, D. S.; Clancy, Y. L.; Lobkovsky, E. B.; Yaghi, O. M.; Dai, S. *Angew. Chem., Int. Ed.* **2006**, *45*, 1390. (b) Li, J.-R.; Kuppler, R. J.; Zhou, H.-C. *Chem. Soc. Rev.* **2009**, *38*, 1477. (c) Li, J.-R.; Sculley, J.; Zhou, H.-C. *Chem. Rev.* **2012**, *112*, 869. (d) Xiang, S.-C.; Zhang, Z.; Zhao, C.-G.; Hong, K.; Zhao, X.; Ding, D.-R.; Xie, M.-H.; Wu, C.-D.; Das, M. C.; Gill, R.; Thomas, K. M.; Chen, B. *Nat. Commun.* **2011**, *2*, 204. (e) Sumida, K.; Rogow, D. L.; Mason, J. A.; McDonald, T. M.; Bloch, E. D.; Herm, Z. R.; Bae, T.-H.; Long, J. R. *Chem. Rev.* **2012**, *112*, 724. (f) Bloch, E. D.; Queen, W. L.; Krishna, R.; Zadrozny, J. M.; Brown, C. M.; Long, J. R. *Science* **2012**, *335*, 1606. (g) Zhang, Z.; Zhao, Y.; Gong, Q.; Li, Z.; Li, J. *Chem. Commun.* **2013**, 49, 653.
- (6) (a) Alaerts, L.; Séguin, E.; Poelman, H.; Thibault-Starzyk, F.; Jacobs, P. A.; De Vos, D. E. *Chem.—Eur. J.* **2006**, *12*, 7353. (b) Seo, J. S.; Whang, D.; Lee, H.; Jun, S. I.; Oh, J.; Jeon, Y. J.; Kim, K. *Nature* **2000**, *404*, 982. (c) Lee, J.; Farha, O. K.; Roberts, J.; Scheidt, K. A.;

- Nguyen, S. T.; Hupp, J. T. *Chem. Soc. Rev.* **2009**, *38*, 1450. (d) Ma, L.; Abney, C.; Lin, W. *Chem. Soc. Rev.* **2009**, *38*, 1248. (e) Zhang, X.; Llabrés i Xamena, F. X.; Corma A. *J. Catal.* **2009**, *265*, 155. (f) Hwang, Y. K.; Hong, D.-Y.; Chang, J.-S.; Jhung, S. H.; Seo, Y.-K.; Kim, J.; Vimont, A.; Daturi, M.; Serre, C.; Férey, G. *Angew. Chem., Int. Ed.* **2008**, *47*, 4144. (g) Yoon, M.; Srirambalaji, R.; Kim, K. *Chem. Rev.* **2012**, *112*, 1196. (h) Gascon, J.; Corma, A.; Kapteijn, F.; Llabrés i Xamena, F. X. *ACS Catal.* **2013**, *4*, 361. (i) Wang, C.; Zheng, M.; Lin, W. *J. Phys. Chem. Lett.* **2011**, *2*, 1701. (j) Zhu, C.; Yuan, G.; Chen, X.; Yang, Z.; Cui, Y. *J. Am. Chem. Soc.* **2012**, *134*, 8058. (k) Mo, K.; Yang, Y.; Cui, Y. *J. Am. Chem. Soc.* **2014**, *136*, 1746. (l) Genna, D. T.; Wong-Foy, A. G.; Matzger, A. J.; Sanford, M. S. *J. Am. Chem. Soc.* **2013**, *135*, 10586. (m) Srirambalaji, R.; Hong, S.; Natarajan, R.; Yoon, M.; Hota, R.; Kim, Y.; Ho, K. Y.; Kim, K. *Chem. Commun.* **2012**, *48*, 11650. (n) Kong, G.-Q.; Ou, S.; Zou, C.; Wu, C.-D. *J. Am. Chem. Soc.* **2012**, *134*, 19851. (o) Ingleson, M. J.; Barrio, J. P.; Bacsá, J.; Dickinson, C.; Park, H.; Rosseinsky, M. J. *Chem. Commun.* **2008**, 1287. (p) Dau, P. V.; Cohen, S. M. *Chem. Commun.* **2013**, *49*, 6128. (q) Fei, H.; Shin, J.; Meng, Y. S.; Adelhardt, M.; Sutter, J.; Meyer, K.; Cohen, S. M. *J. Am. Chem. Soc.* **2014**, *136*, 4965. (r) Zhao, M.; Ou, S.; Wu, C.-D. *Acc. Chem. Res.* **2014**, *47*, 1199.
- (7) (a) Evans, O. R.; Lin, W. *Acc. Chem. Res.* **2002**, *35*, 511. (b) Wang, C.; Zhang, T.; Lin, W. *Chem. Rev.* **2012**, *112*, 1084.
- (8) (a) Allendorf, M. D.; Houk, R. J. T.; Andruszkiewicz, L.; Talin, A. A.; Pikarsky, J.; Choudhury, A.; Gall, K. A.; Hesketh, P. J. *J. Am. Chem. Soc.* **2008**, *130*, 14404. (b) Lan, A.; Li, K.; Wu, H.; Olson, D. H.; Emge, T. J.; Ki, W.; Hong, M.; Li, J. *Angew. Chem., Int. Ed.* **2009**, *48*, 2334. (c) Lu, G.; Hupp, J. T. *J. Am. Chem. Soc.* **2010**, *132*, 7832. (d) Kreno, L. E.; Leong, K.; Farha, O. K.; Allendorf, M.; Van Duyne, R. P.; Hupp, J. T. *Chem. Rev.* **2012**, *112*, 1105. (e) Hu, Z.; Deibert, B. J.; Li, J. *Chem. Soc. Rev.* **2014**, *43*, 5815. (f) Xie, Z.; Ma, L.; deKrafft, K. E.; Jin, A.; Lin, W. *J. Am. Chem. Soc.* **2009**, *132*, 922.
- (9) (a) Della Rocca, J.; Lin, W. *Eur. J. Inorg. Chem.* **2010**, 3725. (b) Della Rocca, J.; Liu, D.; Lin, W. *Acc. Chem. Res.* **2011**, *44*, 957. (c) deKrafft, K. E.; Boyle, W. S.; Burk, L. M.; Zhou, O. Z.; Lin, W. *J. Mater. Chem.* **2012**, *22*, 18139.
- (10) (a) Horcajada, P.; Serre, C.; Vallet-Regí, M.; Sebban, M.; Taulelle, F.; Férey, G. *Angew. Chem., Int. Ed.* **2006**, *45*, 5974. (b) Horcajada, P.; Serre, C.; Maurin, G.; Ramsahye, N. A.; Balas, F.; Vallet-Regí, M.; Sebban, M.; Taulelle, F.; Férey, G. *J. Am. Chem. Soc.* **2008**, *130*, 6774. (c) Rieter, W. J.; Pott, K. M.; Taylor, K. M. L.; Lin, W. *J. Am. Chem. Soc.* **2008**, *130*, 11584. (d) An, J.; Geib, S. J.; Rosi, N. L. *J. Am. Chem. Soc.* **2009**, *131*, 8376. (e) Taylor-Pashow, K. M. L.; Rocca, J. D.; Xie, Z.; Tran, S.; Lin, W. *J. Am. Chem. Soc.* **2009**, *131*, 14261. (f) Horcajada, P.; Chalati, T.; Serre, C.; Gillet, B.; Sebrie, C.; Baati, T.; Eubank, J. F.; Heurtaux, D.; Clayette, P.; Kreuz, C.; Chang, J.-S.; Hwang, Y. K.; Marsaud, V.; Bories, P.-N.; Cynober, L.; Gil, S.; Férey, G.; Couvreur, P.; Gref, R. *Nat. Mater.* **2010**, *9*, 172. (g) Horcajada, P.; Gref, R.; Baati, T.; Allan, P. K.; Maurin, G.; Couvreur, P.; Férey, G.; Morris, R. E.; Serre, C. *Chem. Rev.* **2012**, *112*, 1232. (h) Huxford, R. C.; deKrafft, K. E.; Boyle, W. S.; Liu, D.; Lin, W. *Chem. Sci.* **2012**, *3*, 198. (i) He, C.; Lu, K.; Liu, D.; Lin, W. *J. Am. Chem. Soc.* **2014**, *136*, 5181.
- (11) (a) Kobayashi, Y.; Jacobs, B.; Allendorf, M. D.; Long, J. R. *Chem. Mater.* **2010**, *22*, 4120. (b) Givaja, G.; Amo-Ochoa, P.; Gomez-Garcia, C.; Zamora, F. *Chem. Soc. Rev.* **2012**, *41*, 115. (c) Gándara, F.; Uribe-Romo, F. J.; Britt, D. K.; Furukawa, H.; Lei, L.; Cheng, R.; Duan, X.; O'Keefe, M.; Yaghi, O. M. *Chem.—Eur. J.* **2012**, *18*, 10595. (d) Narayan, T. C.; Miyakai, T.; Seki, S.; Dincă, M. *J. Am. Chem. Soc.* **2012**, *134*, 12932. (e) Sheberla, D.; Sun, L.; Blood-Forsythe, M. A.; Er, S.; Wade, C. R.; Brozek, C. K.; Aspuru-Guzik, A.; Dincă, M. *J. Am. Chem. Soc.* **2014**, *136*, 8859. (f) Yoon, M.; Suh, K.; Natarajan, S.; Kim, K. *Angew. Chem., Int. Ed.* **2013**, *52*, 2688.
- (12) (a) Kent, C. A.; Mehl, B. P.; Ma, L.; Papanikolas, J. M.; Meyer, T. J.; Lin, W. *J. Am. Chem. Soc.* **2010**, *132*, 12767. (b) Kent, C. A.; Liu, D.; Ma, L.; Papanikolas, J. M.; Meyer, T. J.; Lin, W. *J. Am. Chem. Soc.* **2011**, *133*, 12940. (c) Wang, C.; Xie, Z.; deKrafft, K. E.; Lin, W. *J. Am. Chem. Soc.* **2011**, *133*, 13445. (d) Zhang, T.; Lin, W. *Chem. Soc. Rev.* **2014**, *43*, 5982.
- (13) (a) Ma, L.; Falkowski, J. M.; Abney, C.; Lin, W. *Nat. Chem.* **2010**, *2*, 838. (b) Song, F.; Wang, C.; Falkowski, J. M.; Ma, L.; Lin, W. *J. Am. Chem. Soc.* **2010**, *132*, 15390. (c) Falkowski, J. M.; Sawano, T.; Zhang, T.; Tsun, G.; Chen, Y.; Lockard, J. V.; Lin, W. *J. Am. Chem. Soc.* **2014**, *136*, 5213. (d) Cho, S.-H.; Ma, B.; Nguyen, S. T.; Hupp, J. T.; Albrecht-Schmitt, T. E. *Chem. Commun.* **2006**, 2563.
- (14) (a) Manna, K.; Zhang, T.; Lin, W. *J. Am. Chem. Soc.* **2014**, *136*, 6566. (b) Manna, K.; Zhang, T.; Carboni, M.; Abney, C. W.; Lin, W. *J. Am. Chem. Soc.* **2014**, *136*, 13182.
- (15) (a) Cavka, J. H.; Jakobsen, S.; Olsbye, U.; Guillou, N.; Lamberti, C.; Bordiga, S.; Lillerud, K. P. *J. Am. Chem. Soc.* **2008**, *130*, 13850. (b) Kandiah, M.; Nilsen, M. H.; Usseglio, S.; Jakobsen, S.; Olsbye, U.; Tilsted, M.; Larabi, C.; Quadrelli, E. A.; Bonino, F.; Lillerud, K. P. *Chem. Mater.* **2010**, *22*, 6632. (c) Schaate, A.; Roy, P.; Godt, A.; Lippke, J.; Waltz, F.; Wiebcke, M.; Behrens, P. *Chem.—Eur. J.* **2011**, *17*, 6643.
- (16) (a) Vermoortele, F.; Ameloot, R.; Vimont, A.; Serre, C.; De Vos, D. *Chem. Commun.* **2011**, *47*, 1521. (b) Li, L.; Tang, S.; Wang, C.; Lv, X.; Jiang, M.; Wu, H.; Zhao, X. *Chem. Commun.* **2014**, *50*, 2304. (c) Fei, H.; Cohen, S. M. *Chem. Commun.* **2014**, *50*, 4810.
- (17) Here we define the activities of MOF catalysts based on total turnover numbers (TONs) rather than turnover frequencies (TOFs).
- (18) Simmons, E. M.; Hartwig, J. F. *J. Am. Chem. Soc.* **2010**, *132*, 17092.
- (19) (a) Tamao, K.; Ishida, N.; Tanaka, T.; Kumada, M. *Organometallics* **1983**, *2*, 1694. (b) Jones, G. R.; Landais, Y. *Tetrahedron* **1996**, *52*, 7599. (c) Ihara, H.; Sugino, M. *J. Am. Chem. Soc.* **2009**, *131*, 7502.
- (20) Denmark, S. E.; Sweis, R. F. *Acc. Chem. Res.* **2002**, *35*, 835.
- (21) Hartwig, J. F. *Acc. Chem. Res.* **2012**, *45*, 864.
- (22) Li, Q.; Driess, M.; Hartwig, J. F. *Angew. Chem., Int. Ed.* **2014**, *53*, 8471.
- (23) (a) Iverson, C. N.; Smith, M. R. *J. Am. Chem. Soc.* **1999**, *121*, 7696. (b) Ishiyama, T.; Takagi, J.; Ishida, K.; Miyaura, N.; Anastasi, N. R.; Hartwig, J. F. *J. Am. Chem. Soc.* **2002**, *124*, 390. (c) Cho, J.-Y.; Tse, M. K.; Holmes, D.; Maleczka, R. E.; Smith, M. R. *Science* **2002**, *295*, 305. (d) Ishiyama, T.; Takagi, J.; Hartwig, J. F.; Miyaura, N. *Angew. Chem., Int. Ed.* **2002**, *41*, 3056. (e) Roosen, P. C.; Kallepalli, V. A.; Chattopadhyay, B.; Singleton, D. A.; Maleczka, R. E.; Smith, M. R. *J. Am. Chem. Soc.* **2012**, *134*, 11350. (f) Mazzacano, T. J.; Mankad, N. P. *J. Am. Chem. Soc.* **2013**, *135*, 17258. (g) Preshlock, S. M.; Ghaffari, B.; Maligres, P. E.; Krska, S. W.; Maleczka, R. E.; Smith, M. R. *J. Am. Chem. Soc.* **2013**, *135*, 7572. (h) Obligation, J. V.; Semproni, S. P.; Chirik, P. J. *J. Am. Chem. Soc.* **2014**, *136*, 4133.
- (24) (a) Miyaura, N.; Suzuki, A. *Chem. Rev.* **1995**, *95*, 2457. (b) Hayashi, T.; Yamasaki, K. *Chem. Rev.* **2003**, *103*, 2829. (c) Maleczka, R. E.; Shi, F.; Holmes, D.; Smith, M. R. *J. Am. Chem. Soc.* **2003**, *125*, 7792. (d) Holmes, D.; Chotana, G. A.; Maleczka, R. E.; Smith, M. R. *Org. Lett.* **2006**, *8*, 1407. (e) Kudo, N.; Perseghini, M.; Fu, G. C. *Angew. Chem., Int. Ed.* **2006**, *45*, 1282. (f) Murphy, J. M.; Liao, X.; Hartwig, J. F. *J. Am. Chem. Soc.* **2007**, *129*, 15434. (g) Tzschucke, C. C.; Murphy, J. M.; Hartwig, J. F. *Org. Lett.* **2007**, *9*, 761. (h) Beck, E. M.; Hatley, R.; Gaunt, M. J. *Angew. Chem., Int. Ed.* **2008**, *47*, 3004. (i) Wan, L.; Dastbaravardeh, N.; Li, G.; Yu, J.-Q. *J. Am. Chem. Soc.* **2013**, *135*, 18056.
- (25) Yinghuai, Z.; Chenyan, K.; Peng, A. T.; Emi, A.; Monalisa, W.; Kui-Jin Louis, L.; Hosmane, N. S.; Maguire, J. A. *Inorg. Chem.* **2008**, *47*, 5756.
- (26) Tagata, T.; Nishida, M.; Nishida, A. *Adv. Synth. Catal.* **2010**, *352*, 1662.
- (27) (a) Kawamorita, S.; Ohmiya, H.; Hara, K.; Fukuoka, A.; Sawamura, M. *J. Am. Chem. Soc.* **2009**, *131*, 5058. (b) Grüning, W. R.; Siddiqi, G.; Safonova, O. V.; Copéret, C. *Adv. Synth. Catal.* **2014**, *356*, 673. (c) Wu, F.; Feng, Y.; Jones, C. W. *ACS Catal.* **2014**, *4*, 1365.